

# Articles

## Chitosan Graft Copolymer Nanoparticles for Oral Protein Drug Delivery: Preparation and Characterization

Feng Qian,<sup>†,‡</sup> Fuying Cui,<sup>†,‡</sup> Jieying Ding,<sup>†,‡</sup> Cui Tang,<sup>†</sup> and Chunhua Yin<sup>\*,†</sup>

State Key Laboratory of Genetic Engineering, Department of Pharmaceutical Sciences, and Department of Biochemistry, School of Life Sciences, Fudan University, Shanghai 200433, China

Received January 22, 2006; Revised Manuscript Received June 1, 2006

Several novel functionalized graft copolymer nanoparticles consisting of chitosan (CS) and the monomer methyl methacrylate (MMA), *N*-dimethylaminoethyl methacrylate hydrochloride (DMAEMC), and *N*-trimethylaminoethyl methacrylate chloride (TMAEMC), which show a higher solubility than chitosan in a broader pH range, have been prepared by free radical polymerization. The nanoparticles were characterized in terms of particle size, zeta potential, TEM, and FT-IR. These nanoparticles were 150–280 nm in size and carried obvious positive surface charges. Protein-loaded nanoparticles were prepared, and their maximal encapsulation efficiency was up to 100%. In vitro release showed that these nanoparticles provided an initial burst release followed by a slowly sustained release for more than 24 h. These graft copolymer nanoparticles enhanced the absorption and improved the bioavailability of insulin via the gastrointestinal (GI) tract of normal male Sprague–Dawley (SD) strain rats to a greater extent than that of the phosphate buffer solution (PBS) of insulin.

### Introduction

Nanoparticles have been studied extensively as carriers for oral drug delivery, which aim to improve the bioavailability of drugs with poor absorption characteristics.<sup>1</sup> In particular, much attention has been paid to the nanoparticles made of hydrophobic or amphiphilic polymers such as poly- $\epsilon$ -caprolactone (PCL), polylactide (PLA), and poly (lactide-*co*-glycolide) (PLGA) due to their good biocompatibility, biodegradability, and ability to prolong drug release behavior. However, these nanoparticles are not ideal carriers for hydrophilic drugs such as peptide, protein, and DNA drugs because these polymers are not suitable for the absorption of hydrophilic ionic drugs due to their obvious hydrophobic property.<sup>2</sup> To increase the hydrophilicity of a particle surface, many different hydrophilic nanoparticles have been developed as hydrophilic drug carriers. Among those hydrophilic systems, the chitosan nanoparticle is a type of promising carrier for hydrophilic drugs due to its hydrophilic property and other outstanding physicochemical and biological properties.

Chitosan is a (1,4)-linked 2-amino-2-deoxy- $\beta$ -D-glucan and can be obtained from chitin, a kind of waste material from the ocean food industry, by alkaline or enzymatic deacetylation. This natural polysaccharide possesses useful characteristics such as nontoxicity, high biocompatibility, and nonantigenicity that offer advantages for the possibility of clinical use.<sup>3</sup> From the view of biopharmaceutics, chitosan has a special feature of adhering to the mucosal surface and transiently opening the tight junction between epithelial cells. It has been proven that chitosan could enhance the absorption of a drug crossing human intestinal

epithelial (Caco-2) cells without injuring them.<sup>4,5</sup> In recent years, chitosan nanoparticles have been investigated as drug delivery systems for anticancer drugs or protein.<sup>6,7</sup> Several research groups have explored the potential of chitosan as polycationic gene carriers. Chitosan has been shown to effectively combine DNA in saline or acetic acid solution and partially protects DNA from nuclease degradation.<sup>8–10</sup>

Despite all these properties, chitosan is still a polymer that lacks good solubility at physiological pH values. Chitosan has an apparent  $pK_a$  of 5.5, as measured by potentiometric titration. The solubility of chitosan is poor when the pH value is above 6, and it will lose charge when precipitating from solution, indicating that it is unsuitable for ionic absorption in neutral and physiological environments. Recent studies have shown that only protonated soluble chitosan can trigger the opening of the tight junction and facilitate the paracellular transport of hydrophilic compounds.<sup>11</sup> The pH values of the intestinal lumen are close to the  $pK_a$  of chitosan, which limits the efficiency of chitosan as an absorption enhancer. For that reason, chitosan may not be a suitable carrier for targeting protein drugs to specific sites of the intestine. To overcome these drawbacks, many studies have been done. Thanou et al.<sup>12</sup> prepared the nanoparticles that consisted of quaternized chitosan derivatives using *N*-trimethyl chitosan chloride (TMC), and the nanoparticles were able to enhance the intestinal permeation of hydrophilic macromolecular drugs such as peptides and proteins. Xu et al.<sup>13</sup> developed *N*-(2-hydroxyl) propyl-3-trimethylammonium chitosan chloride (HTCC) nanoparticles prepared by the ionic interaction between HTCC and sodium tripolyphosphate (TPP), and the nanoparticles showed a great protein encapsulation efficiency and sustained release ability. However, many organic solvents and high-energy sources were required for the preparation of these nanoparticles, which was disadvantageous to bioactive macromolecules.

\* Corresponding author. Tel: +86-21-6564 3797; fax: +86-21-5552 2771; e-mail: chyin@fudan.edu.cn.

<sup>†</sup> Department of Pharmaceutical Sciences.

<sup>‡</sup> Department of Biochemistry.

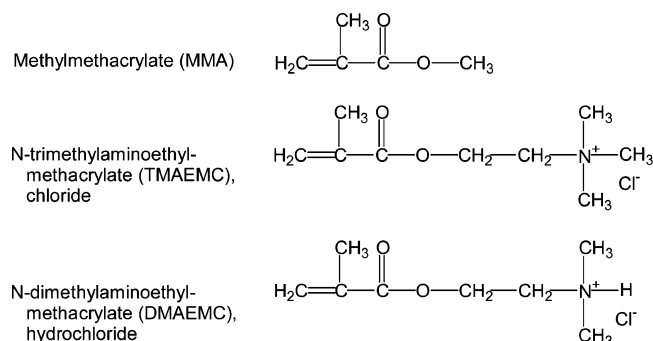


**Figure 1.** Chemical structures of different monomers used for preparation of graft copolymer nanoparticles.

Up to now, injection is the only approach for the therapy of insulin-dependent diabetes mellitus. However, conventional subcutaneous injection treatment does not result in normal physiological daily concentrations of insulin in blood and target tissues, and the patient compliance is not satisfactory. Oral delivery is the most convenient and desired way for drug delivery, especially when repeated or routine administration is necessary. Many researchers believe that oral delivery would be an effective method for protein drugs, which could be easier to perform and lead to improved patient compliance.<sup>14</sup>

In the present study, a novel approach to prepare several hydrophilic nanoparticles consisting of chitosan and the monomer methyl methacrylate (MMA), *N*-trimethylaminoethyl methacrylate chloride (TMAEMC), and *N*-dimethylaminoethyl methacrylate hydrochloride (DMAEMC) (Figure 1) based on free radical polymerization is described. These nanoparticles show higher solubility than chitosan nanoparticles in a broader pH range. The major goal is to prepare novel nanoparticles and to evaluate their potential for protein delivery. The physicochemical properties of these nanoparticles were analyzed by FTIR, photon correlation spectroscopy (PCS), zeta potential analysis, and transmission electron microscopy (TEM). Insulin was designated as the model protein. Insulin-loaded nanoparticles were prepared without any organic solvents and high-energy sources and characterized for their encapsulation efficiency and in vitro release behavior. The effect of nanoparticles on enhancing the intestinal absorption of insulin was studied by measuring the change of the plasma glucose levels at different time points following oral administration.

## Experimental Procedures

**Materials.** Chitosan (deacetylation degree was 85%, 1000 kDa) from crab shells was purchased from Sigma (St. Louis, MO). Methyl methacrylate (MMA), *N*-trimethylaminoethyl methacrylate chloride (TMAEMC), and *N*-dimethylaminoethyl methacrylate hydrochloride (DMAEMC) (Fluka, Bushs, Switzerland) were used as monomers. Ammonium persulfate (APS) was purchased from Sigma (St. Louis, MO). Insulin (27.6 IU/mg) was obtained from Xuzhou biochemical plant (Xuzhou, China). All the other reagents were analytical grade. Male Sprague–Dawley (SD) strain rats of 200–220 g weight were provided by the Animal Center Care Center, Fudan University. The study protocol was reviewed and approved by the Institutional Animal Care and Use Committee, Fudan University, China.

**Preparation of Nanoparticles.** Chitosan–methyl methacrylate (CM) nanoparticles were prepared by free radical polymerization of chitosan and methyl methacrylate. Briefly, chitosan was dissolved to a concentration of 1% (w/v) in 250 mM acetic acid solution under gentle heat, and the pH of the stock solution was adjusted to 4.0. Then, the MMA was added. This mixture was heated to 70 °C under stirring at 500 rpm in a sealed flask of 100 mL. The polymerization process was

triggered by the addition of APS (0.03% w/v) and terminated after 24 h. The obtained nanoparticles were dialyzed in demineralized water for 48 h through a semipermeable membrane with an exclusion size of 10 kDa (Dialysis Tubing–Visking, Medicell, London, UK) and then lyophilized.

Chitosan–*N*-trimethylaminoethyl methacrylate chloride–methyl methacrylate (CTM) and chitosan–*N*-dimethylaminoethyl methacrylate hydrochloride–methyl methacrylate (CDM) nanoparticles were obtained by graft polymerization of CS, TMAEMC, or DMAEMC and MMA. Chitosan and APS (0.045% w/v) were dissolved in 95 mL of 250 mM acetic acid solution under magnetic stirring. The amount of chitosan was maintained constantly at 1% (w/v) in all experiments. When the solution became clear, 1% (w/v) TMAEMC or DMAEMC was added to the solution with continued stirring. The pH of the system was maintained at about 4.0. The polymerization was carried out at 70 °C under nitrogen stream and stirring at 500 rpm. After 1 h, 1% (w/v) of MMA was added. When the opalescent suspension appeared, the reaction system was cooled, and the opalescent suspension was dialyzed in demineralized water for 48 h.

Protein-loaded nanoparticle suspensions were simply prepared by adding the insulin solution into nanoparticle suspensions without any organic solvents and high-energy sources. The phosphate buffer solution of insulin (1 mg/mL) and nanoparticle suspensions (10 or 20 mg/mL, pH 7.4) were preheated to 37 °C separately. An equal volume of both solutions was quickly mixed together and incubated for 3 h at 37 °C. Then, the protein-loaded nanoparticle suspensions could be used in following studies.

**Particle Size.** The particle size of the resulting nanoparticles was determined by photon correlation spectroscopy (PCS) with a BI 90 particle sizer (Brookhaven Instruments Corp., Holtsville, NY). A total of 0.5 mL of nanoparticle suspensions was diluted to 20 mL and measured at 25 °C. The particle size was expressed by mean effective diameter, and the width of size distribution was characterized by the polydispersity index.

Transmission electron microscopy (TEM) of nanoparticles and insulin-loaded nanoparticles was performed by negative staining with phosphotungstic acid. Briefly, a drop of suspension (20 mg/mL) was placed on a Formvar-coated copper grid (150 mesh, Ted Pella Inc., Redding, CA). Excess liquid was removed, and a drop of 2% (w/v) phosphotungstic acid was added to the grid. After 3 min of incubation at room temperature, excess liquid was removed, and the grid was air-dried. The dried grid containing the nanoparticles was visualized using a H-600A transmission electron microscope (Hitachi, Tokyo, Japan).

**Surface Charge.** The zeta potential of each nanoparticle formulation was determined by microelectrophoresis with a Zeta Plus, zeta potential analyzer (Brookhaven Instruments Corp., Holtsville, NY). The zeta potential was measured through diluting a sample of formulation with demineralized water in a ratio of 1:40. All results were transformed to standard values at a reference temperature of 20 °C.

**FTIR Spectrum Analysis.** Infrared absorption spectra of CS, CS-TMAEMC, and CTM nanoparticles were studied by FTIR (M series, Midac Corp.). CS-TMAEMC and CTM nanoparticles were frozen by liquid nitrogen and lyophilized by a freeze-dryer system and then were mixed with KBr and pressed to a plate for measurement, respectively.

**Stability of Nanoparticles in the Solution of Different pH Values.** For determination of the stability profiles, 5 mg of CM, CDM, or CTM nanoparticles was dispersed into 20 mL solutions in a range of pH 2–12, respectively, and these formulations were observed whether suspension or sedimentation occurred at different time points.

**Encapsulation Efficiency and In Vitro Release of Insulin.** The amount of insulin loaded in different nanoparticles was determined by measuring the difference between the total amount of insulin added into nanoparticle suspensions and the amount of nonloaded insulin remaining in the clear supernatant after the loading process. For this purpose, nanoparticle suspensions were ultracentrifuged at 15 000 rpm under 25 °C for 30 min, and then the amount of free insulin in the clear supernatant was determined by the Lowry method<sup>15</sup> using the

supernatant of their corresponding blank nanoparticles as a basic correction. The insulin concentration used during the loading process was 0.5 mg/mL. The encapsulation efficiency was calculated as

encapsulation efficiency =  $(A - B)/A \times 100\%$ , where  $A$  is the total amount of insulin and  $B$  is the amount of nonloaded insulin.

Insulin released from the nanoparticles was determined by incubating the nanoparticles in 1 mL of pH 7.4 PBS at 37 °C. To assess sink conditions for insulin, the concentrations of nanoparticles in the release medium were adjusted to 10 mg/mL. At appropriate time intervals, the individual sample was ultracentrifuged, and the amount of insulin in the supernatant was measured by the Lowry method.

**In Vivo Studies.** Normal male Sprague–Dawley (SD) strain rats (six per group) of 200–220 g weight were fasted for 12 h before used. Insulin-loaded nanoparticles were administered orally at a dose of 100 IU/kg of body weight: (1) insulin-loaded CM nanoparticles, (2) insulin-loaded CDM nanoparticles, (3) insulin-loaded CTM nanoparticles, and (4) subcutaneous injection of insulin (1 IU/kg). All the previous formulations were dispersed in a medium of pH 7.4 PBS before administration. As a control, a PBS solution of insulin was administered to rats under the same conditions.

Blank plasma samples were obtained from the tail vein of the rats prior to oral administration to establish baseline glucose levels. At appropriate time intervals after oral administration, plasma samples were obtained in the same way. The glucose level in the plasma sample was measured using the glucose–oxidase method (Glucose GOD-PAD kit, Shanghai Kexin Biotech Institute, Shanghai, China). Results were shown as the mean plasma glucose levels ( $\pm$ standard deviation) of rats in the same group.

**Statistical Analysis.** The plasma glucose levels determined in blank plasma samples were taken as the baseline levels, and the mean plasma glucose levels and standard errors for all samples were determined. Values from different groups were compared with the control groups by the Students *t*-test, and *P* values of 0.05 or less were considered significant.

## Results and Discussion

**Preparation of Nanoparticles.** A redox initiator is usually used in graft copolymerization because of its high efficiency. There are some reports that persulfate can combine a redox system to initiate the copolymerization of vinyl monomers, and APS has been used to initiate the graft copolymerization of chitosan.<sup>16,17</sup> Figure 2 shows that the initiator of the APS and  $\text{NH}_2$  group of chitosan combined a redox system and initiated the graft copolymerization of chitosan and MMA, DMAEMC, or TMAEMC by generating free radicals in the macromolecules. These graft copolymers consisting of hydrophilic chitosan-DMAEMC or chitosan-TMAEMC, and the hydrophobic MMA chains spontaneously formed nanoparticles in water. The hydrophobic segment will be condensed to a core in the water, and the hydrophilic segment will enwrap the hydrophobic core to form nanoparticles. The proportion of the hydrophobic segment in the grafted polymers exceeds that of the hydrophilic segment, so the grafted polymers could form the particles in the water. If the grafted polymers were added to the hydrophobic organic solvents, the polymers could not form the nanoparticles but form individual polymer chains. In the experiment of preparation, the opalescent suspension appeared, which indicated that the nanoparticles had been formed. These nanoparticles carrying obvious positive surface charges resulted in stronger repulsion between the positive chains of nanoparticles, so the polymers could only form a network with difficulty. These nanoparticle suspensions were dialyzed in demineralized water for 48 h, lyophilized, and then gravimetrically analyzed, which resulted in a yield of about 85% of the total polymerized materials.

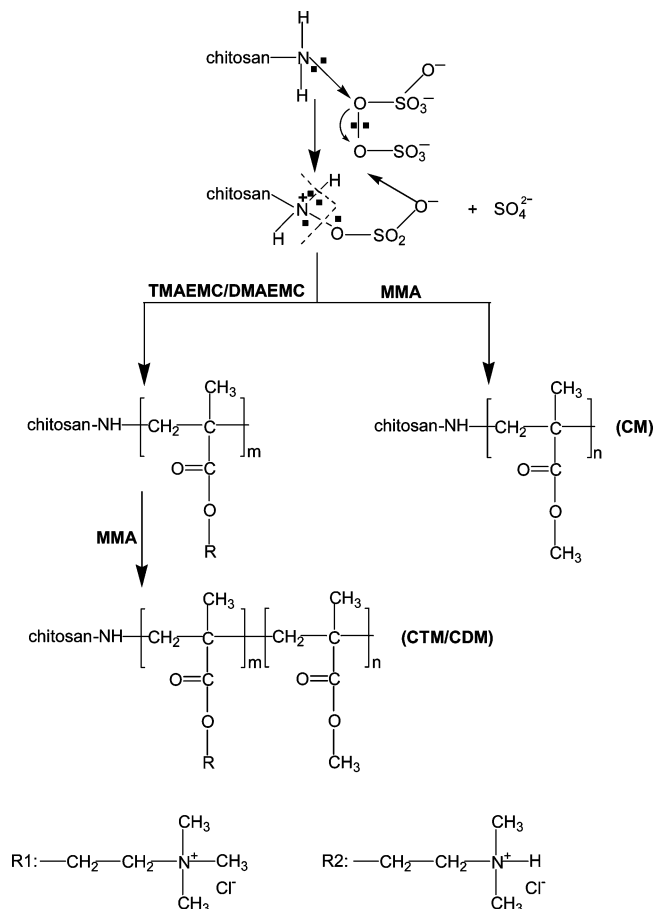


**Figure 2.** Reaction schemes of CM, CDM, and CTM nanoparticles.

**Table 1.** Particle Size and Surface Charge of Different Nanoparticles ( $n = 6$ )

nanoparticles	mean diameter (nm)	PCS <sup>a</sup>	zeta potential (mV)
CM	156.4 $\pm$ 6.2 (0.045)		17.2 $\pm$ 3.3
CDM	232.6 $\pm$ 5.5 (0.089)		21.8 $\pm$ 0.7
CTM	271.1 $\pm$ 6.5 (0.083)		29.4 $\pm$ 0.7

<sup>a</sup> Values in parentheses represent the polydispersity index.

The insulin-loaded nanoparticles formed as a result of complex ionic interactions between insulin and nanoparticles. The cationic characteristic of the nanoparticles is the crucial parameter for the complex formation. In pH 7.4, the anionic insulin can be spontaneously adsorbed by the surface of the nanoparticles with a positive charge.

**Particle Size and Surface Charge.** The mean diameters of nanoparticles determined by PCS were shown in Table 1. The polydispersity indexes were inferior to 0.1, indicating that the nanoparticles had a narrow size distribution. Zeta potentials (surface charge) measured in demineralized water are shown in Table 1. CM, CDM, and CTM nanoparticles were characterized by obvious positive potentials. CTM nanoparticles had a stronger zeta potential of about 30 mV due to the cationic functional group of  $-\text{N}^+(\text{CH}_3)_3$  of TMAEMC.

Transmission electron micrographs (TEM) of nanoparticles and insulin-loaded nanoparticles were shown in Figure 3. Nanoparticles are generally monodispersed spheres having a solid and consistent structure (Figure 3A,C,E). The powdered nanoparticles can be easily dispersed to form a suspension by rehydrating. Figure 3B illustrated that insulin-loaded CM nanoparticles were agglomerated and led to a larger particle size ( $>300$  nm). Insulin-loaded CDM and insulin-loaded CTM



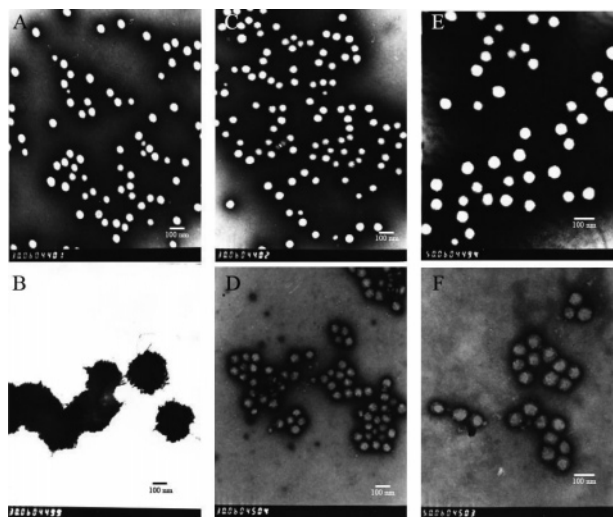


**Figure 3.** TEM of (A) CM, (C) CDM, and (E) CTM nanoparticles and (B) insulin-loaded CM, (D) insulin-loaded CDM, and (F) insulin-loaded CTM nanoparticles stained by phosphotungstic acid. Bar represents 100 nm.

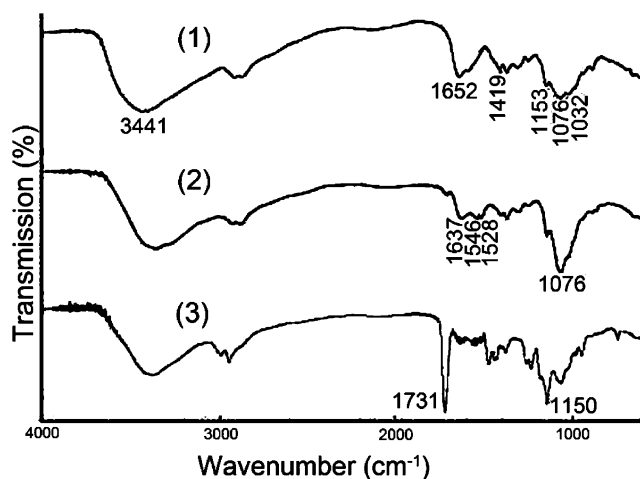


**Figure 4.** FTIR of (1) chitosan, (2) chitosan-TMAEMC, and (3) CTM nanoparticles.

nanoparticles shown in Figure 3D,F had a circular shape consisting of a dark shell and a light core. These results indicated that insulin was loaded in the hydrophilic chains of the nanoparticle surface, and then the loaded insulin and nanoparticles formed the core-shell structure.

**FTIR Spectrum Analysis.** Figure 4 shows the results of FTIR spectra of chitosan, chitosan-TMAEMC, and CTM nanoparticles. The spectrum of chitosan showed peaks assigned to saccharide structures at 1153, 1076, 1032, and 897  $\text{cm}^{-1}$ , and two strong amino characteristic peaks at around 3441, 1652, and 1325  $\text{cm}^{-1}$  were assigned to the amide I and III bands, respectively. The peak at 1419  $\text{cm}^{-1}$  was the joint contribution of the bend vibration of OH and CH.<sup>17</sup> Compared with chitosan, chitosan-TMAEMC showed that the absorption peak became stronger at 1076  $\text{cm}^{-1}$ , which was attributed to the increase on the C—O group of TMAEMC. The NH-associated band at the peak at 1652  $\text{cm}^{-1}$  disappeared, and a new peak at 1637  $\text{cm}^{-1}$  appeared, which can be assigned to the absorption peak of the ammonium of TMAEMC. The two new peaks at 1546 and 1528  $\text{cm}^{-1}$  that appeared could be attributed to the carboxylate of TMAEMC. Furthermore, the grafted polymers were analyzed via  $^1\text{H}$  NMR after lyophilization, and chitosan-TMAEMC polymer showed a strong resonance signal at about 3.3—(—N<sup>+</sup>—

**Table 2.** Effect of Concentration of Nanoparticles on Insulin Encapsulation Efficiency<sup>a</sup>

nanoparticles	encapsulation efficiency (%)	
	5 <sup>b</sup>	10 <sup>b</sup>
CM	19.6	60.6
CDM	80.1	96.9
CTM	85.7	100

<sup>a</sup> Insulin 0.5 mg/mL,  $n = 3$ . <sup>b</sup> Concentration of nanoparticles (mg/mL).

( $\text{CH}_3$ )<sub>3</sub> ppm (data not shown). These results confirmed that TMAEMC had been associated to the  $\text{NH}_2$  of chitosan, which were consistent with the results of other modified chitosan.<sup>2, 13</sup> For CTM nanoparticles, a new strong peak appeared at 1731  $\text{cm}^{-1}$  that indicated the incorporation of the carbonyl of MMA, and a characteristic peak at 1150  $\text{cm}^{-1}$  suggested the introduction of alkyl groups of MMA. Figure 4 indicated that chitosan-TMAEMC and CTM nanoparticles had been prepared.

**Stability of Nanoparticles in the Solution of Different pH Values.** The effect of pH value on the stability of nanoparticles was investigated in macrography. CM nanoparticles were sedimentated above pH 7 within 30 min, and CDM nanoparticles were agglomerated above pH 11 within 1 h and sedimentated within 2 h. However, CTM nanoparticles were dispersed in the range of pH 2 to 12 in more than 1 month without any agglomerate occurring. The functional group of —N<sup>+</sup>(CH<sub>3</sub>)<sub>3</sub> of TMAEMC was not protonated or deprotonated in acid or alkaline solution, and the positive zeta potential of the CTM nanoparticles was maintained at 25–30 mV, which led to a stable nanoparticle suspension in a broader pH range.

**Encapsulation Efficiency and In Vitro Release of Insulin.** In most nanoparticle delivery systems, the drug carrying capacity is defined as an encapsulation efficiency. In the present study, insulin was carried on the nanoparticles via the ionic interaction between insulin and positive hydrophilic chains of nanoparticles. In water, the long hydrophilic chains extended to the water, and some insulin might be encapsulated among the positive hydrophilic chains, which indicated that the insulin was not only on the surface of the nanoparticles but also was distributed in the outer hydrophilic area. So, the insulin carrying capacity of the nanoparticles could be termed as encapsulation efficiency. As shown in Table 2, the encapsulation efficiencies of the CDM and CTM nanoparticles were higher than those of the CM nanoparticles due to their stronger positive surface charges. The loading efficiency increased with the initial concentration level of the nanoparticle raise. Increasing the concentration of nanoparticles from 5 to 10 mg/mL increased the encapsulation efficiency of insulin from 19.6 to 60.6% for CM, 80.1 to 96.6% for CDM, and 85.7 to 100% for CTM nanoparticles, respectively. The CM, CDM, or CTM nanoparticles had a positive surface charge more or less. Protein loading studies carried out at different pH values indicated that, for insulin, the greatest encapsulation efficiency was obtained when the insulin was dissolved at a pH above its isoelectric point, so that the protein was predominantly negatively charged.<sup>18</sup> This suggested that the mechanism of loading of insulin to nanoparticles was partially mediated by an ionic interaction between insulin and positive hydrophilic chains of nanoparticles. This mechanism was also supported by the observed neutralization of the surface charge of nanoparticles due to the loading of increasing amount of insulin.<sup>19</sup> Taking into account that the isoelectric point of insulin is 5.3, insulin-loaded nanoparticles were prepared in a phosphate buffer solution at pH 7.4, which favors the interaction between insulin and the CM, CDM, and CTM nanoparticles and then results in a high encapsulation efficiency.

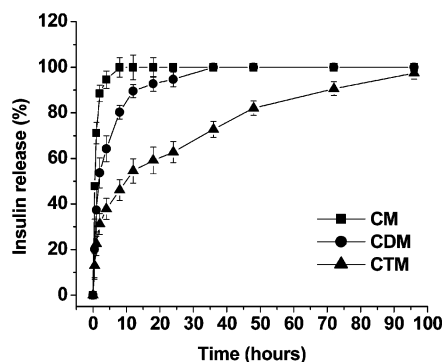


**Figure 5.** Release profiles of insulin from CM, CDM, and CTM nanoparticles in pH 7.4 phosphate buffer solution at 37 °C (mean  $\pm$  SD,  $n = 6$ ).

The preliminary *in vitro* release behavior of insulin from CDM or CTM nanoparticles had indicated that they had a sustained release form. Figure 5 shows the release profiles of insulin from CM, CDM, and CTM nanoparticles in PBS (pH 7.4) at 37 °C. Nearly all the loaded insulin was completely released from CM nanoparticles in 6 h. An initial burst release followed by a slowly sustained release of insulin occurred in the CDM or CTM nanoparticles. Moreover, these nanoparticles provided a continuous release of the loaded insulin for up to 1 or 4 days. The mechanism of the release was the diffusion of associated insulin from nanoparticles. The results indicated that the release rate was highly affected by the interactive force between loaded-insulin and surface chains of nanoparticles. The surface charge of CTM was stronger than those of the CM and CDM nanoparticles, and the ionic interactive force was larger, so the dissociation of associated insulin governing the release process was slow. On the other hand, the release of protein also depended on the pH values of the release medium. The release profile at pH 4.5 showed the slowest release rate, while the nanoparticles barely had any sustained release property at pH 2.0 (data not shown). The results were coincident with the conclusion drawn by Hu et al.<sup>2</sup> The changed release rate could be a result of the changed solubility of insulin and the different interactions between insulin and nanoparticles in the different release medium.

**In Vivo Studies.** The potential of these nanoparticles as carriers that improve the absorption and bioavailability of insulin via the GI tract was examined by measuring the plasma glucose levels after oral administration of insulin-loaded nanoparticles. The actual glucose values were used typically in hypoglycemic effects of diabetic model rats but not normal SD rats. In the present study, the percent of plasma glucose levels could indicate the hypoglycemic effect of insulin-loaded nanoparticles and be compared to that of the control group. The plasma glucose level decreased slightly after oral administration of the insulin PBS solution at a dose of 100 IU/kg (Figure 6), which indicated that only a small amount of active insulin was absorbed due to the low membrane permeability of insulin and degradation of the majority of insulin caused by proteases. As shown in Figure 6, a significantly prolonged decline of the plasma glucose level was obtained over 10 h after administration of the insulin-loaded nanoparticles at a dose of 100 IU/kg of body weight. CM, CDM, or CTM nanoparticles reduced glucose levels by 10–20, 20–30, or 30–40%, respectively. These results indicated that insulin was released from nanoparticles in its active form and that the bioavailability was improved by these nanoparticles.

Most of the protein drugs would be destroyed by the harsh conditions of the GI tract before reaching the bloodstream. In the case of insulin, less than 0.1% of the oral dosed insulin

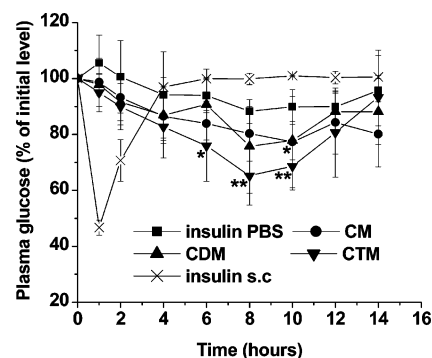


**Figure 6.** Plasma glucose levels achieved in SD rats following oral administration of insulin PBS solution, insulin-loaded CM nanoparticles, insulin-loaded CDM nanoparticles, insulin-loaded CTM nanoparticles, and subcutaneous injection of insulin in PBS (1 IU/kg). Each dose of insulin in the nanoparticle suspension was 100 IU/kg of body weight (mean  $\pm$  SD,  $n = 6$  per group). Statistically significant difference from control (\* $P < 0.05$  and \*\* $P < 0.01$ ).

reached the bloodstream intact.<sup>14</sup> The particulate system had the properties to enhance the absorption and improve the bioavailability of insulin in the GI tract. Longer et al.<sup>20</sup> were the first to show that a delayed GI transit induced by polymers could lead to an increased oral drug bioavailability. Takeuchi et al.<sup>21</sup> reported that the chitosan-coated insulin-loaded liposomes after oral administration could reduce blood glucose levels of rats by about 30%, and the decreasing blood glucose level could be maintained up to 12 h.

Nanoparticles made of muco-adhesive materials such as chitosan could adhere to the mucous layer and transiently open the tight junctions between the epithelial cells, where the drug is released from the nanoparticles slowly. The increase of residence time and drug concentration in the vicinity of the epithelial cells through intensifying the intimate contact of the drug with the mucous layer could significantly improve the degree of drug absorption.<sup>22</sup> In the GI tract, the cationic nanoparticles prefer to bind to the mucous layer with a negative charge.<sup>23</sup> The stronger positive surface charge of the CTM nanoparticles resulted in stronger interactions with the mucous layer, which led to further absorption enhancement of insulin.

Besides, an explanation of this absorption enhancement of insulin could be the ability of nanoparticles to offer some assurance of the stability of insulin and to protect it from degradation in the harsh conditions of the GI tract. The protein was protected by nanoparticles due to the physicochemical interaction between enzyme and hydrophilic chains of the nanoparticle surface. Enzymes were captured by nanoparticles physicochemically so that the amount of free enzymes decreased in the GI tract and so this decrease helped the stabilization of the protein.<sup>24</sup> The competition for the surface binding sites of the enzymes with insulin might exist, but the results of the hypoglycemic effect indicated that some insulin was transported to the intestine and absorbed into the blood. In *in vivo* studies, the nanoparticles were reasonably excessive in the mixture, and the enzyme would be absorbed to blank nanoparticles. So, the effect of competition for surface binding sites of the enzymes with insulin was limited, and most of insulin could transport to the small intestine. These demonstrated that the nanoparticles having the properties stated previously would be useful carriers for oral insulin delivery.

## Conclusion

In conclusion, several hydrophilic nanoparticles consisting of chitosan and different monomers can be prepared based on

free radical polymerization. These nanoparticles have narrow size distributions and positive surface charges. CM nanoparticles are stable in pH 2–7, CDM nanoparticles are stable in pH 2–10, and CTM nanoparticles are dispersed in the range of pH 2–12 without any agglomerate. A high encapsulation efficiency of insulin has been obtained, and the in vitro release profiles of insulin from CDM and CTM nanoparticles show an initial burst release followed by a slowly sustained release phase. Increasing the surface charge of the nanoparticles improves insulin encapsulation efficiency and slows the release. The in vivo studies indicate that CDM and CTM nanoparticles seem to be a very promising vehicle for oral administration of hydrophilic proteins and peptides. In further studies, the cytotoxicity and muco-adhesion of these different nanoparticulate carriers will be studied.

**Acknowledgment.** The authors are thankful for the financial support from Science and Technology Commission of the Shanghai Municipality of China (054319934).

## References and Notes

- (1) Florence, A. T.; Hillery, A. M.; Hussain, N.; Jani, P. U. *J. Controlled Release* **1995**, *36*, 39–46.
- (2) Hu, Y.; Jiang, X. Q.; Ding, Y.; Ge, H. X.; Yuan, Y. Y.; Yang, C. Z. *Biomaterials* **2002**, *23*, 3193–3201.
- (3) Polk, A.; Amsden, B.; De Yao, K.; Peng, T.; Doosen, M. F. A. *J. Pharm. Sci.* **1994**, *83*, 178–185.
- (4) Artursson, P.; Lindmark, T.; Davis, S. S.; Illum, L. *Pharm. Res.* **1994**, *11*, 1358–1361.
- (5) Schipper, N. G. M.; Varum, K. M.; Artursson, P. *Pharm. Res.* **1996**, *13*, 1686–1692.
- (6) Hari, P. R.; Chandy, T.; Sharma, C. P. *J. Appl. Polym. Sci.* **1996**, *59*, 1795–1801.
- (7) Gupta, K. C.; Kumar, M. N. V. R. *Biomaterials* **2000**, *21*, 1115–1119.
- (8) Roy, K.; Mao, H. Q.; Huang, S. K.; Leong, K. W. *Nat. Med.* **1999**, *5*, 387–391.
- (9) Leong, K. W.; Mao, H. Q.; Truong-Le, V. L. *J. Controlled Release* **1998**, *53*, 183–193.
- (10) Richardson, S. C. W.; Kolbe, H. J. V.; Duncan, R. *Int. J. Pharm.* **1999**, *178*, 231–243.
- (11) Kotzé, A. F.; Lueßen, H. L.; De Boer, A. G.; Verhoef, J. C.; Junginger, H. E. *Eur. J. Pharm. Sci.* **1998**, *7*, 145–151.
- (12) Thanou, M. M.; Kotzé, A. F.; Scharringhausen, T.; Lueßen, H. L.; De Boer, A. G.; Verhoef, J. C.; Junginger, H. E. *J. Controlled Release* **2000**, *64*, 15–25.
- (13) Xu, Y. M.; Du, Y. M.; Huang, R. H.; Gao, L. P. *Biomaterials* **2003**, *24*, 5015–5022.
- (14) Foss, A. C.; Goto, T.; Morishita, M.; Peppas, N. A. *Eur. J. Pharm. Biopharm.* **2004**, *57*, 163–169.
- (15) Peterson, P. L. *Anal. Biochem.* **1977**, *83*, 346–356.
- (16) Sun, T.; Xu, P. X.; Liu, Q.; Xue, J.; Xie, W. M. *Eur. Polym. J.* **2003**, *39*, 189–192.
- (17) Xie, W. M.; Xu, P. X.; Wang, W. *Carbohydr. Polym.* **2002**, *50*, 35–40.
- (18) Calvo, P.; Remunan, C.; Vial, J. L.; Alonso, M. J. *J. Appl. Polym. Sci.* **1997**, *63*, 125–132.
- (19) Janes, K. A.; Calvo, P.; Alonso, M. J. *Adv. Drug Delivery Rev.* **2001**, *47*, 83–97.
- (20) Longer, M. A.; Ch'ng, H. S.; Robinson, J. R. *J. Pharm. Sci.* **1985**, *74*, 406–411.
- (21) Takeuchi, H.; Yamamoto, H.; Kawashima, Y. *Adv. Drug Delivery Rev.* **2001**, *47*, 39–54.
- (22) Kreuter, J.; Muller, U.; Munz, K. *Int. J. Pharm.* **1989**, *55*, 39–45.
- (23) Sakuma, S.; Suzuki, N.; Kikuchi, H. *Int. J. Pharm.* **1997**, *149*, 93–106.
- (24) Sakuma, S.; Hayashi, M.; Akashi, M. *Adv. Drug Delivery Rev.* **2001**, *47*, 21–37.

BM060065F